

Cell Reports, Volume 30

Supplemental Information

Domain Model Explains Propagation

Dynamics and Stability of Histone H3K27

and H3K36 Methylation Landscapes

Constance Alabert, Carolin Loos, Moritz Voelker-Albert, Simona Graziano, Ignasi Forné, Nazaret Reveron-Gomez, Lea Schuh, Jan Hasenauer, Carsten Marr, Axel Imhof, and Anja Groth

Figure S1

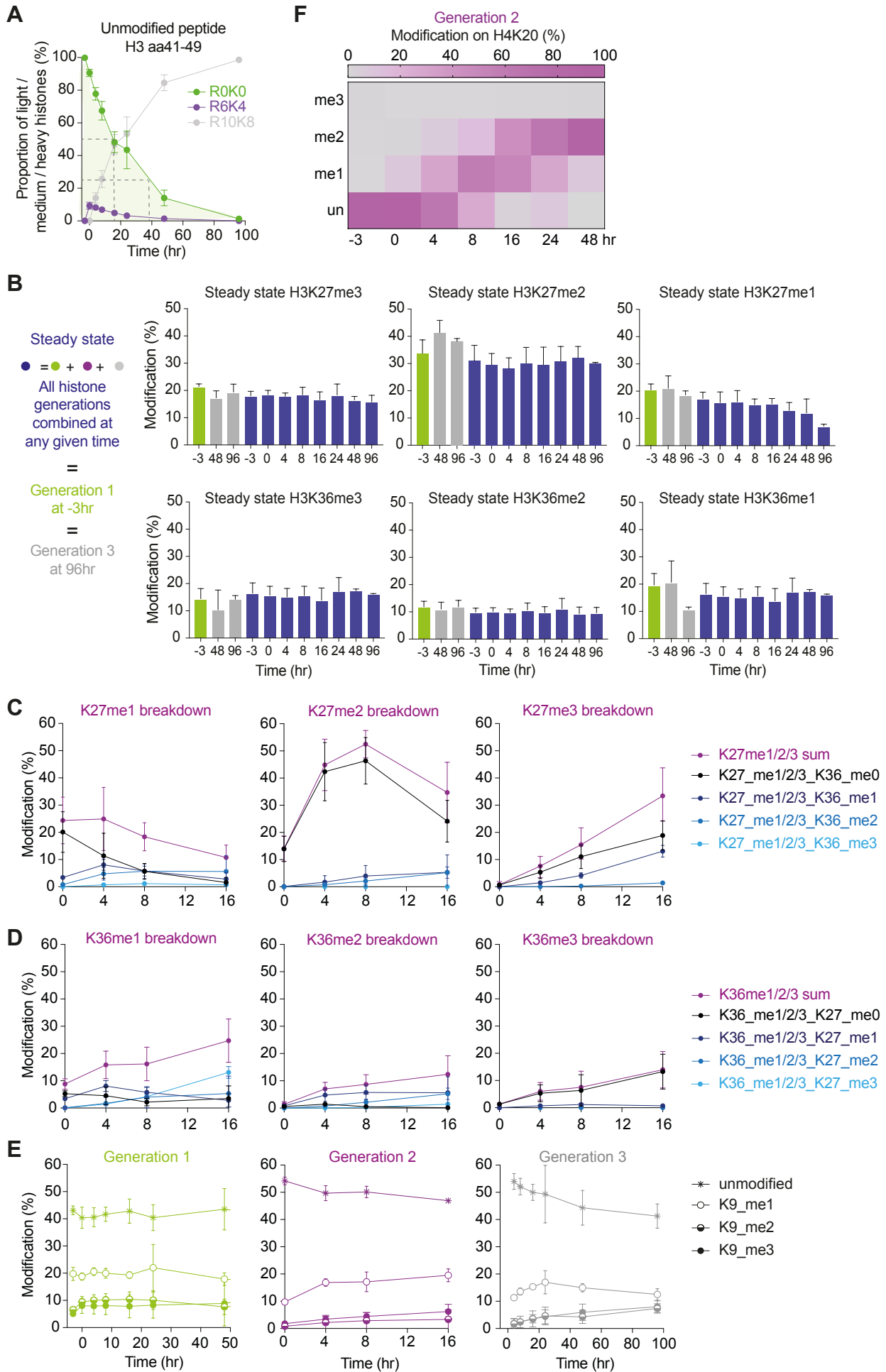


Figure S1, related to Figure 1. **A.** Proportion of each histone generations across the time course, based on quantification of the H3 aa41-49 peptide that remains unmodified. The proportion is given as a percentage such that the sum equals 100 % at any given time. **B.** Total modification levels across the time course, represented by pre-existing histones (green), combinations of the different generations (blue) and third generation histones (grey). For each modification, the sum is given (e.g. for K27me3 is given as the sum of K27me3K36me0, K27me3K36me1, K27me3K36me2, and K27me3K36me3). **C, D.** Methylation levels on generation 2 histones for K27 and K36, on all individual peptides used to generate the sum shown in Fig. 1D. **E.** Methylation levels on histone generations 1, 2 and 3 for H3K9. (un) unmodified; (me1) mono-methylated; (me2) di-methylated; (me3) tri-methylated. **F.** Heatmap showing stepwise methylation of H4K20 methylation on generation 2 histones. (un) Unmodified; (me1) mono-methylated; (me2) di-methylated; (me3) tri-methylated.

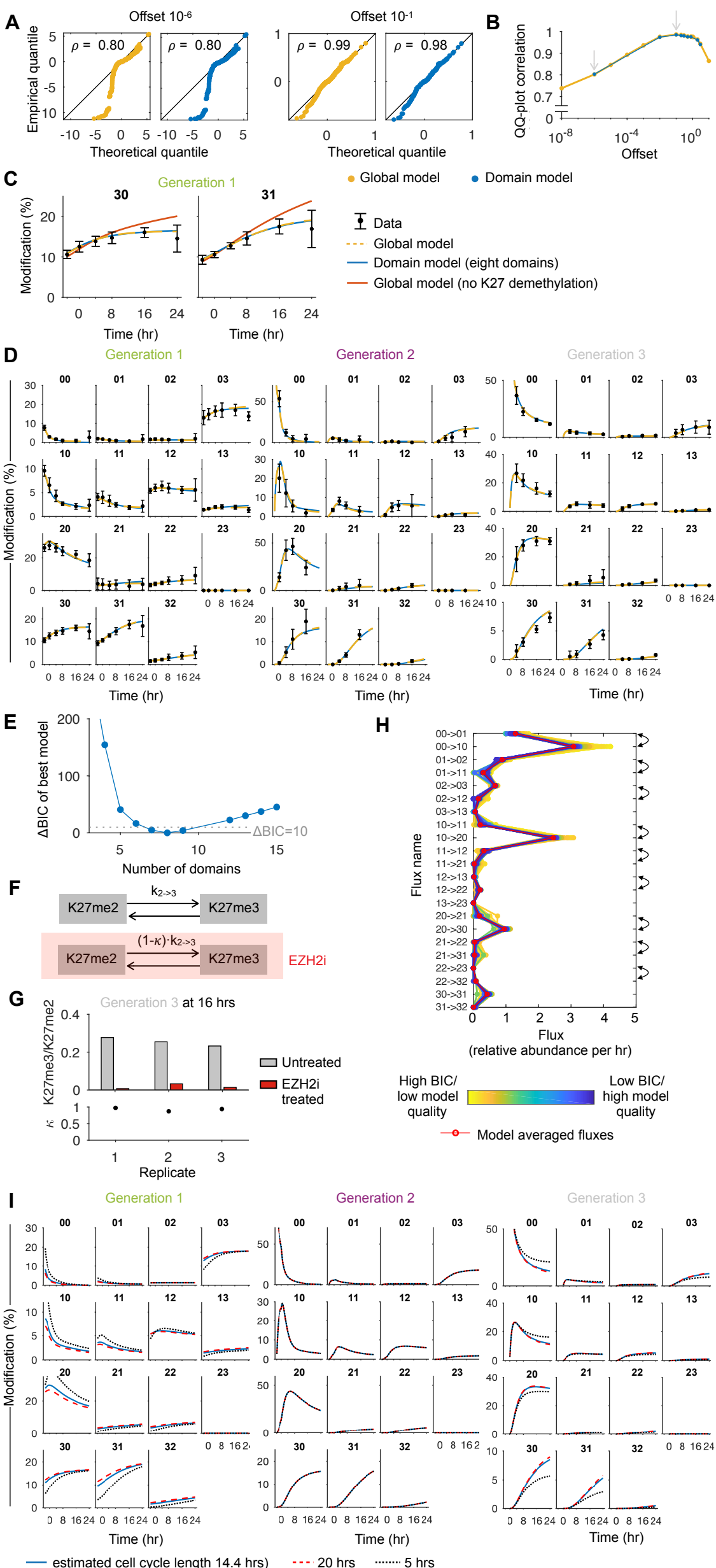
Figure S2

Figure S2, related to Figure 2. **A.** Comparing different offsets by which data and model simulation are shifted shows highest QQ correlations for 10^{-1} . **B.** Correlation for the QQ-plots for varying offsets. The maximum correlation is achieved for offset 10^{-1} . **C.** Model fits including the global model without K27 demethylation for K27me3K36me0 and K27me3K36me1. The models were calibrated for the full data set. **D.** Both the global and the domain model is able to fit methylation dynamics in all generations. **E.** Model reduction for the domain model. The difference in BIC values is shown for the best tested model with given numbers of domains. A model with 8 domains has the best Bayesian Information Criterion (BIC) value, and there are models with 7 and 9 domains which cannot be rejected according to their BIC value. The dotted line shows the threshold of $\Delta\text{BIC}=10$. **F.** Illustration of the parametrization for the efficiency κ of the inhibitor. **G.** Estimates for κ comparing K27me3 and K27me2 levels for generation 3 histones for untreated cells and cells with EZH2 inhibitor. **H.** Fluxes obtained with the maximum likelihood estimates (MLEs) for all calibrated models. The models are color coded according to their BIC value. The model averaged (using BIC weights) fluxes are highlighted with red and fluxes which are compared in Fig. 2F are highlighted by arrows. **I.** Prediction of methylation dynamics for varying cell cycle lengths using the domain model. The blue line indicates the model for the estimated cell cycle length of 14.4 hrs. For a faster cell cycle (5 hrs, black dotted line), the model predicts overall a higher relative abundance of the lower methylated states, while for a slower cell cycle (20 hrs, red dashed line) the overall relative methylation slightly increases. The initial methylation abundances for generation 1 histones differ for the cell cycle lengths, but approach the same steady state when the cell cycle does not affect the dynamics anymore (after 0 hr). For histones of generation 2, the cell cycle length only has an influence during the 3 hrs labeling time and, therefore, the differences for different cell cycle lengths are minor. Histones of generation 3 approach different population steady states for varying cell cycle lengths.

Figure S3

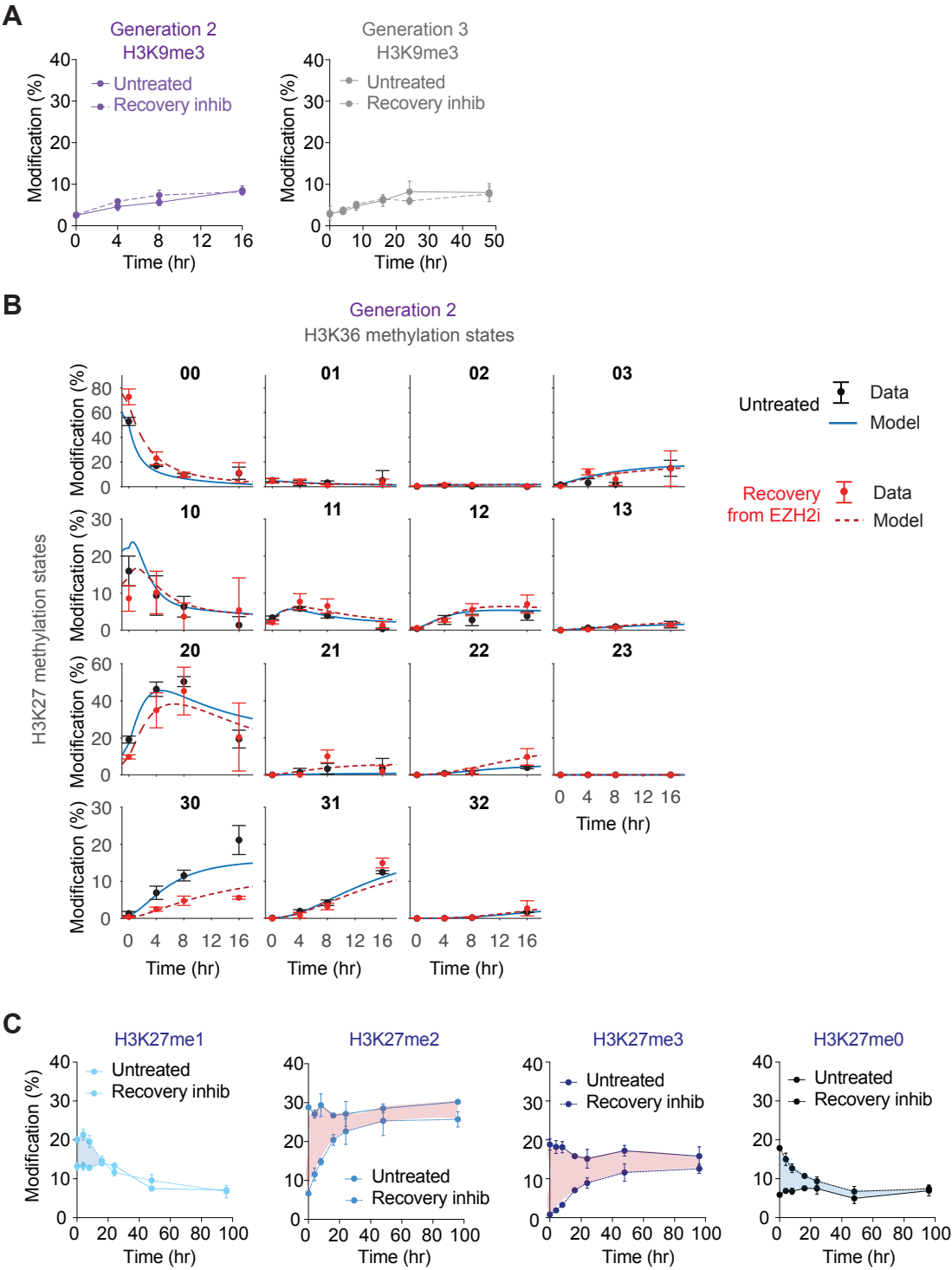
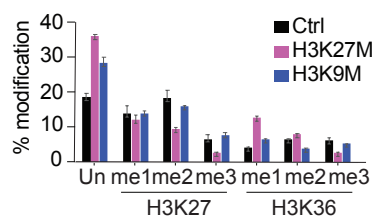


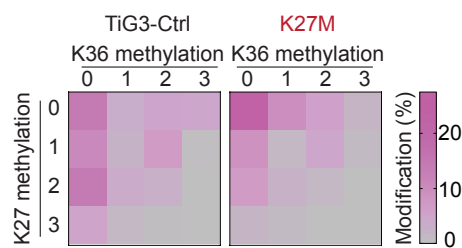
Figure S3, related to Figure 3. **A.** H3K9me3 levels on generation 2 and 3 histones. Experimental design as described in Fig. 3B. **B.** K27 and K36 methylation levels on generation 2 histones for untreated cells and during recovery. Experimental measurements and the model fit allowing for differences in the methylation rate constants $k_{00 \rightarrow 01}$, $k_{00 \rightarrow 10}$, $k_{20 \rightarrow 21}$ and $k_{20 \rightarrow 30}$ are shown. **C.** Total methylation levels on K27 across the time course on the combination of all three histone generations calculated as in Fig. S1B. Losses and gains compared to untreated control are by pink and blue shaded areas, respectively.

Figure S4

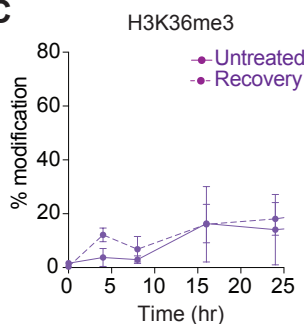
A



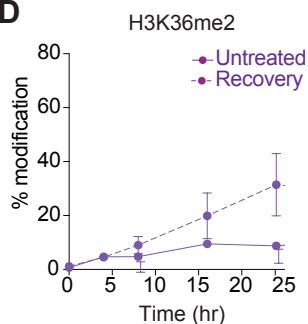
B



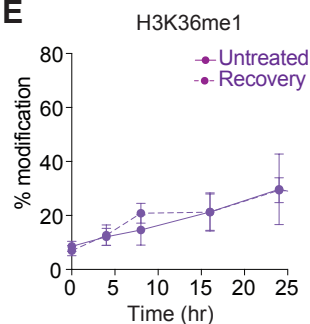
C



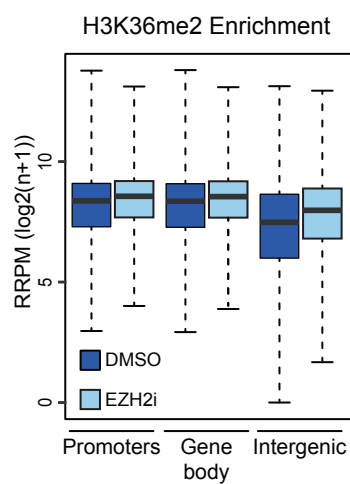
D



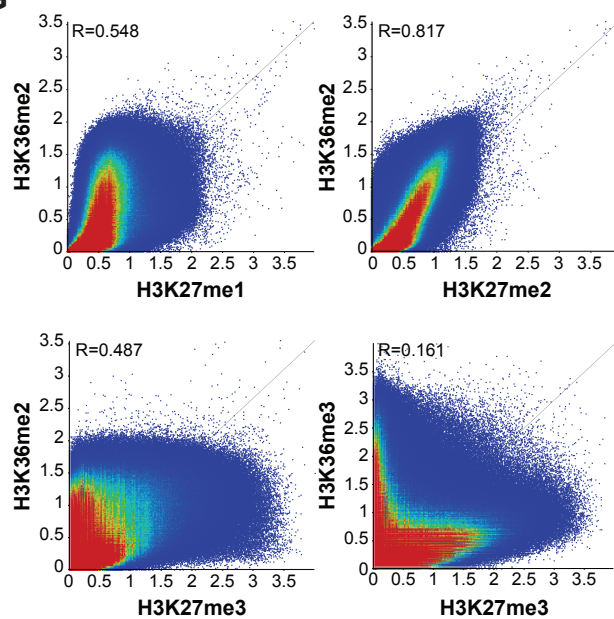
E



F



G



H

H3K36me2 Enrichment at K27me3 domains

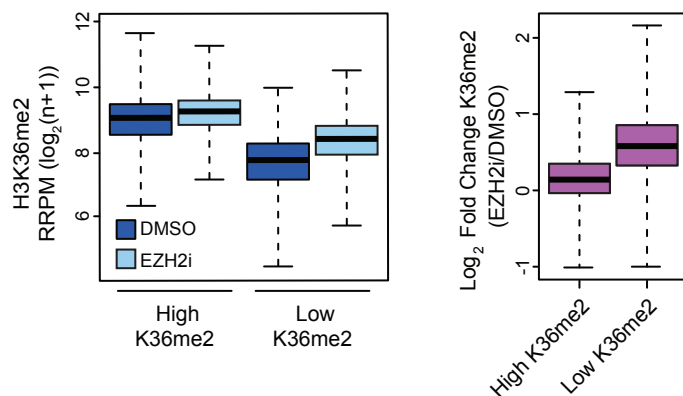


Figure S4, related to Figure 4. **A.** Bar-diagram showing H3K27 and H3K36 methylation levels in TIG-3 cells expressing H3K27M and H3K9M and untransduced controls (Ctrl). **B.** Heatmap showing H3K27 and H3K36 methylation levels in TIG-3 cells expressing H3K27M compare to control (Ctrl). **C-E.** H3K36 methylation levels on generation 2 histones in untreated conditions and upon recovery from EZH2 inhibitor treatment. **F.** Boxplot of H3K36me2 ChIP-seq signal over 1kb windows across promoters, gene bodies and intergenic regions. Black line, median; dashed lines, $1.5 \times$ interquartile range. Quantitated with RRPM, $\log_2(n + 1)$. **G.** Scatterplots showing direct comparison of ChIP-seq signal over 1kb windows across the genome for the indicated pairs of histone modifications. Quantitated with RPM, $\log_2(n+1)$. Pearson's correlation R value for each plot is shown. **H.** Boxplot of H3K36me2 ChIP-seq signal over 1kb windows across H3K27me3 domains overlapping (high K36me2) or not overlapping (low K36me2) K36me2 peaks. Black line, median; dashed lines, $1.5 \times$ interquartile range. Quantitated with RRPM, $\log_2(n + 1)$.

Supplemental Table 1, related to STAR method, LC-MS analysis of histone modifications.

Mass [m/z]	Formula [M]	Formula type	Species	CS [z]	Polarity	Start [min]	End [min]	(N)CE	(N)CE type	MSX ID	Comment
539.3141				3	Positive	35	45	29	NCE		H3_27_40_K27K36K37_m1pp + H3_27_40_K27K36K37_pm1p_light
545.346				3	Positive	35	45	29	NCE		H3_27_40_K27K36K37_m1pp + H3_27_40_K27K36K37_pm1p_medium
550.6644				3	Positive	35	45	29	NCE		H3_27_40_K27K36K37_m1pp + H3_27_40_K27K36K37_pm1p_heavy
529.9825				3	Positive	30	40	30	NCE		H3_27_40_K27K36K37_m2m1p + H3_27_40_K27K36K37_pm3p_light
536.0143				3	Positive	30	40	30	NCE		H3_27_40_K27K36K37_m2m1p + H3_27_40_K27K36K37_pm3p_medium
541.3328				3	Positive	30	40	30	NCE		H3_27_40_K27K36K37_m2m1p + H3_27_40_K27K36K37_pm3p_heavy
534.6544				3	Positive	32	40	30	NCE		H3_27_40_K27S28K36K37_me3me1p + H3_27_40_K27S28K36K37_me1me3p_light
540.6862				3	Positive	32	40	30	NCE		H3_27_40_K27S28K36K37_me3me1p + H3_27_40_K27S28K36K37_me1me3p_medium
546.0047				3	Positive	32	40	30	NCE		H3_27_40_K27S28K36K37_me3me1p + H3_27_40_K27S28K36K37_me1me3p_heavy
525.3106				3	Positive	30	38	30	NCE		H3_27-40_K27K36K37_pme2p + H3_27-40_K27K36K37_me2pp_light
531.3424				3	Positive	30	38	30	NCE		H3_27-40_K27K36K37_pme2p + H3_27-40_K27K36K37_me2pp_medium
536.6609				3	Positive	30	38	30	NCE		H3_27-40_K27K36K37_pme2p + H3_27-40_K27K36K37_me2pp_heavy
520.6509				3	Positive	25	35	32	NCE		H3_27-40_K27K36K37_me2me3p + H3_27-40_K27K36K37_me3me2p_light
526.6827				3	Positive	25	35	32	NCE		H3_27-40_K27K36K37_me2me3p + H3_27-40_K27K36K37_me3me2p_medium
532.0011				3	Positive	25	35	32	NCE		H3_27-40_K27K36K37_me2me3p + H3_27-40_K27K36K37_me3me2p_heavy
543.986				3	Positive	34	42	30	NCE		H3_27_40_K27K36K37_m1m1p_light
550.0178				3	Positive	34	42	30	NCE		H3_27_40_K27K36K37_m1m1p_medium
555.3363				3	Positive	34	42	30	NCE		H3_27_40_K27K36K37_m1m1p_heavy